Colloids and Surfaces B: Biointerfaces 222 (2023) 113044

Contents lists available at ScienceDirect

Colloids and Surfaces B: Biointerfaces

journal homepage: www.elsevier.com/locate/colsurfb

Interaction of polymers with bile salts – Impact on solubilisation and absorption of poorly water-soluble drugs

Claudia Pigliacelli [a,d,*], Peter Belton [b], Peter Wilde [c], Francesca Baldelli Bombelli [d], Paul A. Kroon [c], Mark S. Winterbone [c], Sheng Qi [a,**]

[a] School of Pharmacy, University of East Anglia, Norwich, Norfolk NR4 7TJ, UK
[b] School of Chemistry, University of East Anglia, Norwich, Norfolk NR4 7TJ, UK
[c] Quadram Institute Bioscience, Norwich Research Park, Norwich, Norfolk NR4 7UQ, UK
[d] Dipartimento di Chimica, Materiali ed Ingegneria Chimica "G. Natta", Politecnico di Milano, Via Mancinelli 7, 20131 Milan, Italy

ARTICLE INFO

Keywords:
Bile salts
Biorelevant media
Solid dispersions
HPMC
Poorly water-soluble drugs
Cellular uptake

ABSTRACT

Formulating poorly soluble drugs with polymers in the form of solid dispersions has been widely used for improving drug dissolution. Endogenous surface-active species present in the gut, such as bile salts, lecithin and other phospholipids, have been shown to play a key role in facilitating lipids and poorly soluble drugs solubilisation in the gut. In this study, we examined the possible occurrence of interactions between a model bile salt, sodium taurocholate (NaTC), and model spray dried solid dispersions comprising piroxicam and Hydroxypropyl Methylcellulose (HPMC), a commonly used hydrophilic polymer for solid dispersion preparation. Solubility measurements revealed the good solubilisation effect of NaTC on the crystalline drug, which was enhanced by the addition of HPMC, and further boosted by the drug formulation into solid dispersion. The colloidal behaviour of the solid dispersions upon dissolution in biorelevant media, with and without NaTC, revealed the formation of NaTC-HPMC complexes and other mixed colloidal species. Cellular level drug absorption studies obtained using Caco-2 monolayers confirmed that the combination of drug being delivered by solid dispersion and the presence of bile salt and lecithin significantly contributed to the improved drug absorption. Together with the role of NaTC-HPMC complexes in assisting the drug solubilisation, our results also highlight the complex interplay between bile salts, excipients and drug absorption.

1. Introduction

Effective drug dissolution in the gut is essential for proper drug absorption and subsequent realisation of the pharmacological effect of oral dosage forms [1–3]. The use of polymer-based solid dispersions has been shown to be a valid approach to increase the solubilisation of poorly water-soluble drugs [4–6] and potentially improve their oral bioavailability [7,8]. The fundamental understanding of solid dispersions behaviour, including the manufacturing, characterisation and *in vitro* dissolution in, mostly, non-biorelevant media have extensively been described in the literature [9–11]. More recently, increasing attention has been paid to the physiological parameters that play a role in drug dissolution and absorption processes, to design biorelevant *in vitro* test methods and better achieve *in vivo /in vitro* correlations [9,12–17].

Human gut fluids comprise a wide range of surface-active compounds endowed with emulsification and solubilisation capacities, such as bile salts (BS), lecithin (LT) and other phospholipids, which can substantially increase the amount of hydrophobic molecules effectively solubilised in the gut [18]. In particular, BS are known to play a primary role in facilitating the hydrolysis and solubilisation of lipids during the digestion process and to promote poorly water-soluble drugs dissolution in the gut [15,19–22]. Given their solubilisation capacity, BS have been included, together with phospholipids, as essential components of the first biorelevant media, FaSSIF and FeSSIF, developed in 1998 by Dressman et al. [23] and Galia et al. [24], and progressively used in all the biorelevant media designed in the last decades to mimic physiological solubility [25–27].

Together with their high solubilisation ability, BS have been reported for their tendency to interact with different drug delivery systems, influencing their solubilisation and subsequent drug absorption

* Corresponding author at: School of Pharmacy, University of East Anglia, Norwich, Norfolk NR4 7TJ, UK.
** Corresponding author.
E-mail addresses: claudia.pigliacelli@polimi.it (C. Pigliacelli), sheng.qi@uea.ac.uk (S. Qi).

https://doi.org/10.1016/j.colsurfb.2022.113044
Received 20 July 2022; Received in revised form 1 November 2022; Accepted 18 November 2022
Available online 19 November 2022

behaviour [15,17,28–33]. It is well know that ionic surfactants, such as BS, can have extensive molecular interactions with polymers and other surfactants in colloidal systems [34–42] and pharmaceutical polymers have been reported to impact the gut solubilisation system [43]. However, in the context of polymer-based solid dispersion formulations, this possible solubilisation interplay, *in vitro* and *in vivo,* has not been fully understood. Previous studies from some of us indicated the occurrence of different types of interaction between Hydroxypropyl Methylcellulose (HPMC) and Polyvinylpyrrolidone (PVP) with BS [44], and several research groups have shown that the use of bio-relevant media containing BS affects drug solubilisation and uptake *in vivo,* when a polymer based solid dispersion is used as an excipient or as drug carrier [35,45–48]. Thus, it is reasonable to hypothesize that polymer-BS interactions may play a role in the solubilisation of poorly water-soluble drugs [49]. However, the complex composition of biorelevant media makes the study of molecular interactions between the solid dispersion polymers and specific species within the biorelevant media highly challenging. Therefore, knowledge of the interaction occurring between solid dispersions carrier and each key surface-active compound is needed to achieve a comprehensive understanding of solid dispersion behaviour in biorelevant media.

In this study, we focused on investigating the interactions of a polymeric-based solid dispersions with sodium taurocholate (NaTC), BS used in all the biorelevant media designed to simulate the human small intestine fluids in the fasted and fed states,[42] and on assessing the potential impact on drug absorption using Caco-2 cell culture model. For this purpose, model solid dispersions of HPMC and piroxicam (PXM) were prepared by spray drying. PXM is a non-steroidal anti-inflammatory drug (NSAID), classified as BSC class II drug and described as practically insoluble in water, with a pH-dependent solubility typically lower than 1 mg/mL [50]. BS have been shown to aid the solubilisation of pH-sensitive drugs, preventing their precipitation in the range of gut pH conditions [51]. Given its pH-dependent solubility and its dissolution-rate limited absorption, we reasoned that PXM could represent a good model for assessing the impact of solubilising colloids species formed in bio-relevant conditions on the dissolution and absorption of poorly water-soluble drugs. The solubility enhancement of PXM by the addition of NaTC alone and the combination of NaTC and HPMC was investigated. The impact of HPMC-NaTC interaction on the formation of colloidal and solubilising species was probed by dynamic light scattering (DLS), nanoparticle tracking analysis (NTA) and cryogenic transmission electron microscopy (Cryo-TEM). The cellular response of Caco-2 cell line was used as the preliminary evidence to test the possible influence of non-digestible water-soluble polymers on the cellular uptake of poorly soluble drugs in the presence of BS.

2. Materials and methods

2.1. Materials

HPMC K4M as the polymeric carrier was kindly donated by Colorcon, Dartford Kent, UK. The model drug, PXM, was purchased from Molekula, UK. 75 cm^2 flasks, cells scrapers, 6 and 96-well plates were purchased from Greiner Bio-One, Austria. All the reagents employed were purchased from Sigma-Aldrich unless otherwise stated. Sodium taurocholate (NaTC) with 99 % purity and lecithin (LT) from egg yolk were purchased from Prodotti chimici e alimentari SPA (Bassaluzzo, Italy) and Acros Organics (Geel, Belgium), respectively. Four different model intestinal media were used in this study: fasted state simulating intestinal fluid with (FaSSIF) and without LT (B-FaSSIF), mimicking the intestinal condition before meals, and fed state simulating intestinal fluid with (FeSSIF) and without LT (B-FeSSIF), to reproduce the intestinal environment after meals. The FeSSIF and FaSSIF media were prepared by following the method developed by Dressman et al. [23] and described by Marques [52]. Briefly, the FaSSIF media was prepared using phosphate buffer with a final pH of 6.5, NaTC concentration of 3 mM and LT concentration of 0.75 mM. FeSSIF was prepared using acetate buffer with a final pH of 5, NaTC concentration of 15 mM and LT concentration of 3.75 mM, as summarized in Table 1.

Buffers components concentrations were as follows: for FaSSIF NaOH 8.7 mM, NaH_2PO_4 28.6 mM, NaCl 105.9 mM. For FeSSIF NaOH 20.8 mM, CH_3COOH 28.8 mM, NaCl 40.6 mM. For both buffers pH adjustment was performed.

2.2. Solubility studies of model drug in biorelevant media

The media used in this part of study include pH 6.5 and 5 buffers, B-FaSSIF and B-FeSSIF, FaSSIF and FeSSIF. The saturated drug concentration in these media were measured by adding excess amounts of drug to the test medium until no further drug dissolution could occur. All samples were kept under constant magnetic agitation at 37 °C for 72 h to allow the dissolution process to reach equilibrium. After 72 h, samples were filtered using a syringe filter with 0.45 μm pore size (Fisher Scientific, Loughborough, UK) and, after appropriate dilution, the drug concentration was assayed using a UV–Vis spectrometer (Perkin Elmer, Waltham, Massachusetts, USA). The wavelength of maximum absorbance (λ_{max}) used for PXM was 334 nm. The effects of the polymer on the solubility of the drug in these media were tested by adding HPMC to the media in the range of concentrations, 2–9 mg/mL, prior to adding the drug which was used in the concentration 1 mg/mL. Linearity between absorbance and concentration was tested using PXM at various concentrations and the response was linear with a correlation coefficient $r^2 = 0.9981$ for buffer at pH 6.5 and $r^2 = 0.9993$ for buffer at pH 5.

2.3. Preparation of physical mixtures and drug loaded solid dispersions by spray drying

HPMC and PXM physical mixtures were prepared by gently mixing raw (unprocessed) material powder using mortar and pestle for about 2 min. For spray drying, PXM in ethanol solution was mixed with HPMC dissolved in Milli-Q water, to obtain the spray drying solution for preparing the solid dispersions. The spray drying parameters were set as follows: inlet temperature 85 °C, aspirator setting 100 %, pump setting 5 % (4 mL/min^{-1}). The spray dried placebo and drug loaded formulations with three different w/w drug: polymer ratios (1:2, 1:4, 1:9) were prepared. The outlet temperatures of the spray drying processes of the formulations ranged between 49 and 57 °C (details can be found in Supplementary Material Table S1).

2.4. Formulation characterisation

The features of the obtained spray dried solid dispersions were studied using a range of solid-state characterisation techniques.

Table 1
Media employed in this study.

Media employed in the study	Salt	NaTC concentration	LT concentration
Buffer pH 6.5	Phosphate buffer	–	–
Buffer pH 5	Acetate buffer	–	–
B-FaSSIF	Phosphate buffer	3 mM	–
B-FeSSIF	Acetate buffer	15 mM	–
FaSSIF	Phosphate buffer	3 mM	0.75 mM
FeSSIF	Acetate buffer	15 mM	3.75 mM
B-FaSSIF-2	Phosphate buffer	1.5 mM	0.75 mM
B-FeSSIF-2	Acetate buffer	1.5 mM	0.75 mM
FaSSIF-2	Phosphate buffer	1.5 mM	0.75 mM
FeSSIF-2	Acetate buffer	1.5 mM	0.75 mM

Scanning electron microscopic (SEM) studies were performed using a JSM 4900LV SEM (JEOL Ltd, Tokyo, Japan), fitted with a tungsten filament. A 20 kV acceleration voltage and 10 mm working distance were used. Powder X-Ray diffraction (PXRD) measurements were performed using an Xtra X-Ray diffractometer (Thermo ARL, Thermo Scientific, Waltman, MA). The X-Ray tube, composed of copper, was operated under a voltage of 45 kV and current of 40 mA. The PXRD patterns were recorded from 3° to 60° 2θ at a step of 0.01°/min. Differential scanning calorimetry (DSC) was used to investigate the thermal behaviour of raw materials, spray dried solid dispersions and physical mixtures. A Q2000 DSC and standard aluminium crimped pans (TA Instrument, Newcastle, USA) were used with a scanning rate of 10 ºC/min between − 20 °C and 250 ºC. Attenuated total reflectance-Fourier transformed infrared spectroscopic (ATR-FTIR) studies were performed using a Perkin Elmer Spectrum BXTR-IR (Waltham, Massachusetts, USA) equipped with an attenuated reflectance (ATR) accessory (SPECAC, Orpington, UK). Spectra were collected in absorbance mode and 64 scans were collected for each sample, at a resolution value of 2 cm^{-2}. All experiments were performed in triplicate (n = 3).

2.5. Dynamic light scattering (DLS)

DLS experiments were performed on a Zetasizer Nano ZS, Malvern Instrument, (Malvern, Worcestershire, United Kingdom) fitted with a 633 nm red laser. Sample were prepared by dissolving weighed materials (polymer 0,7 mg, physical mixture 2:1 1 mg, spray dried formulation 2:1 1 mg) in 2.5 mL of medium and subsequently left in magnetic agitation for 1 h at 37 °C. Samples were centrifuged at 2000 g for 10 min, in order to remove dust particles from the scattering volume. Approximately 1 mL of sample was transferred in a disposable cuvette (pathlength 1 cm) and left to reach equilibration for 15 min. The autocorrelation functions were measured at a fixed angle of 173° (Back Scattering detection). Measurements were performed at 37 °C. Each measurement was composed of 5 runs of 1 min and was repeated three times (n = 3). All final hydrodynamic size distributions (intensity-weighted) of the studied aggregates were derived by fitting autocorrelation functions using the CONTIN algorithm.

2.6. Nanoparticle tracking analysis (NTA) measurements

NTA experiments were carried out using a LM10 Nanosight (Nanosight Ltd - Malvern Instruments Ltd, Malvern Worcestershire, United Kingdom), fitted with a 638 nm laser. NTA technique was used to visualize the size distribution of polymer, BS and BS-polymer aggregates in solution. Sample were prepared by dissolving weighed materials (polymer 0.7 mg, physical mixture 2:1 1 mg, spray dried formulation 2:1 1 mg) in 2.5 mL of medium and subsequently leaving them in magnetic agitation for 1 h at 37 °C. Samples were then equilibrated and measured at room temperature. The temperature of each run was measured and taken into consideration when the size calculation was performed by the software. Particle tracking analysis was performed using Nano-tracking Analysis (NTA) software. All samples were analysed in triplicate (n = 3).

2.7. Cryogenic-transmission electron microscopy (Cryo-TEM)

Sample to be imaged by Cryo-TEM were prepared by dissolving appropriately weighed (polymer 0,7 mg, spray dried formulation 2:1 1 mg) solid in 2.5 mL of the studied medium and left in magnetic agitation for 1 h at 37 °C. Samples were centrifuged at 2000 g for 10 min, to remove dust particles, and the supernatant solutions were analysed after 24 h. Cryo-TEM samples were prepared according to the reported routine procedure described briefly as it follows [53]. A small droplet of the sample solution was placed under controlled conditions on a pre-treated Cu grid of about 20 μm thickness, which was covered by a perforated cellulose acetate butyrate film. Excess material was removed by a gentle wiping off with a filter paper. The specimen was vitrified by being rapidly transferred into liquid ethane. Sample examination was performed with a Zeiss 902 A electron microscope operating at 80 kV at 100 K.

2.8. Cytotoxicity studies

For Clonal Caco-2 cells culture see ESI. Cells were cultured in 96-well tissue culture plates at culture conditions described in Section 6.3.2 in 200 μl per well. Once 80 % confluency was reached (approximately 3 weeks), cells were washed twice using pre-warmed sterile PBS. Subsequently 200 μL of test solution samples were added and the cells were placed in the incubator (Napco 4530 water-jacketed CO_2 incubator at 37 ºC with 5 % CO_2 and 95 % air) for two hours. Two type of cytotoxicity tests were conducted, lactate dehydrogenase (LDH) cytotoxicity test and Cyto-Tox Glo™ test. Samples for uptake studies were prepared using autoclaved glassware and buffers. NaTC, LT and spray dried samples were dissolved in the autoclaved buffers, using autoclaved buffers and incubated at 37 °C for 2 h.

The apical release of LDH enzyme was determined using a colorimetric kit following a previously reported method [54]. After two hours of incubation, 100 μL of apical medium was transferred into a clean plate. 50 μL of substrate reagent were added to the samples, 30-minutes of reaction period was allowed at room temperature and the plates were protected from light. After 30 min, 50 μL of stopping solution were added. Absorbance was measured at 492 nm. (Hitachi spectrophotometer, Hitachi High Technologies America, Schaumburg, USA) LDH content was calculated as % of the total LDH content measured by inducing total cell lysing with 0.1 % Triton X-100. The Cyto-Tox Glo™ assay uses a luminogenic peptide, the (alanyl-alanyl-phenylalanyl-aminoluciferin) AAF-Glo™ substrate, to measure the activity of protease released by the dead cells. 100 μL of apical media were transferred into a clean opaque well. 50 μL of the assay reagents were added to each well. The samples were incubated for 30 min at room temperature. After 30 min, luminescence was measured using a FLUOstar OPTIMA microplate reader (BMG Labtech GmbH, Ortenberg, Germany). Meanwhile 100 μL of lysing buffer were added to the original plate and left in oscillation for 10–15 min. 100 μL of apical media were then withdrawn from the original plate containing the lysing buffer and transferred to the opaque plate containing apical media added with assay reagents. Luminescence was measured again after 15 min of oscillation.

2.9. Cellular drug uptake studies

Caco-2 cells were grown in 6-well plates until 21 days post confluence. Samples for uptake studies were prepared using autoclaved glassware and buffers. NaTC, LT and spray dried samples were dissolved in the autoclaved buffers and incubated at 37 °C for 2 h. Before performing uptake study, confluent cells were washed twice using sterile PBS and aspirated. After washing, the cells were treated with 2 mL of sample and placed in the incubator for 2 h. For each sample, 5 replicates were studied. 1 mL of apical media was withdrawn from each well. Cells were then washed twice using sterile PBS and scraped after addition of 400 μL of sterile water. Apical media and scraped cells were collected in sterile eppendorf vials and frozen after addition of 25 μL of ethanol and 25 μL acetic acid for each vial (sample frozen ≈ 1 mL). Samples were later analysed using HPLC analysis. Data analysis was performed by dividing PXM (μg) detected in the cells lysate by the total amount (μg) of drug detected (lysed cells + apical media content). Absorbed PXM was expressed as percentage of total drug load. In this part of the study, all FaSSIF and FeSSIF media were prepared using 1.5 mM of NaTC (named as B-FaSSIF-2 and B-FeSSIF-2) due to the high cytotoxicity of NaTC.

2.10. HPLC analysis of cells absorption samples

Samples collected from absorption and transport studies were firstly defrosted and sonicated for 10 min using a sonication bath. Samples

were subsequently vortexed and centrifuged for 15 min at 15,000 rpm. Supernatant was used for HPLC analysis. In this study, HPLC analysis was carried out in reverse phase with a Perkin Elmer (Waltham, Massachusetts, USA) high performance liquid chromatography having a Series 200 isocratic pump, equipped with a Series 600 link interface and a Series 200 UV–VIS detector. TC-NAV (Perkin Elmer, Waltham, Massachusetts, USA) software was used to collect, integrate and analyse the chromatographic data. UV detection was carried out at 314 nm. A C18 150 × 4.6 mm column Supelco Li-Chrospher, RP18 Sum was used. For the analysis, the mobile phase consisted of HPLC grade acetonitrile (MeCN) - phosphate buffer (40:60 v/v) adjusted to pH 3 with phosphoric acid, at an injection volume of 10 μL and a flow rate of 1 mL min^{-1}. The retention time of PXM was approximately 5.2 min with this system. Linearity between absorbance and concentration was tested using external standards at various concentrations and the response was linear with a correlation coefficient $r^2 = 0.9959$, over the whole range of used concentrations. A standard stock solution of PXM (0.7 mg/mL) in the mobile phase and a series of dilutions with concentration between 0.28 and 0.7 μg/mL were prepared. Each sample was prepared in triplicate and analysed three times.

2.11. Data analysis and statistics

For solubility, drug encapsulation, DSC and DLS results, the standard deviation values are calculated using data obtained from 3 replicates. For cellular cytotoxicity and uptake studies, the standard deviation values calculated using data obtained from 5 replicates are presented. Uptake data are presented as mean values with standard deviation (n = 5). Statistical analysis was performed using one-way ANOVA followed by a Dunnett's test. P-values of less than 0.05 were considered statistically significant.

3. Results and discussion

3.1. The effect of polymer and NaTC on drug solubility

The equilibrium solubility of crystalline PXM in different media was firstly measured in several media, with and without the presence of HPMC and/or NaTC. As shown in Table 2, PXM is more soluble at pH 6.5 than at pH 5 buffer, in agreement with its pKa_1 and pKa_2 values reported in the literature, which are 1.86 and 5.46, respectively [55]. The addition of HPMC significantly increased PXM solubility in pH 6.5 and pH 5 buffers by more than 5 and 3 folds, respectively. Such a solubility enhancement reveals the drug solubilisation role played by the polymer, in agreement with literature data [56–60]. HPMC is known to exhibit self-assembling properties and to interact with hydrophobic and poorly soluble species, attributing to this surfactant-like behaviour its ability to maintain hydrophobic drug molecules at supersaturation [58–62]. Notably, drug solubility values did not vary significantly when HPMC amount was increased up to 4 and 9 mg/mL, indicating a possible saturation of HPMC solubility enhancement effect at concentrations higher than 2 mg/mL.

Table 2
PXM solubility values in different media, with and without the presence of HPMC at 2, 4 and 9 mg/mL at 37 °C. (n = 3).

Medium	PXM apparent solubility values (μg/mL)			
	PXM	HPMC:PXM (HPMC 2 mg/mL)	HPMC:PXM (HPMC 4 mg/mL)	HPMC:PXM (HPMC 9 mg/mL)
Buffer pH 6.5	34.1 ± 0.2	186.2 ± 6.2	233.4 ± 19.5	188.2 ± 3.1
Buffer pH 5	14.5 ± 0.1	55.3 ± 2.8	54.9 ± 8.1	55.4 ± 4.2
B-FaSSIF	41.6 ± 3.6	208.8 ± 1.2	203.5 ± 39.0	196.1 ± 8.2
B-FeSSIF	58.3 ± 8.1	70.8 ± 7.3	77.5 ± 2.3	76.9 ± 2.1
FaSSIF	206.6 ± 19.1	211.9 ± 31.2	226.6 ± 10.2	258.2 ± 1.9
FeSSIF	34.9 ± 3.5	45.2 ± 1.8	45.1 ± 16.2	129.3 ± 2.2

As previously reported by some of us, CMC value of NaTC in the buffers used in this study is approximately 3 mM [44]. Hence, the presence of NaTC micelles is expected to be limited for B-FaSSIF (NaTC concentration 3 mM), while it is definitely relevant in the case of B-FeSSIF (NaTC concentration 15 mM). As seen in Table 2, drug solubility values show a higher increase in B-FeSSIF than in B-FaSSIF, with respect to the solubility values observed in the buffers. Although the presence of NaTC can reduce the fluid surface tension and improve the wetting of the drug powder aggregates, this would only affect the rate of drug dissolution, but not the equilibrium solubility. Thus, the moderate increase of PXM solubility in B-FeSSIF could be attributed to a direct solubilisation mechanism of NaTC, which is in agreement with the literature [63]. Notably, in the presence of HPMC, PXM solubility in B-FaSSIF did not increase significantly (about 10 %) when compared to the values observed in buffer (pH 6.5), suggesting that NaTC 3 mM might be too low to induce interaction with HPMC and affect the drug solubilisation. Differently, in B-FeSSIF, HPMC impact appeared to be more significant, with a PXM solubility increase of about 25 % (from 55.3 to 70.8 μg/mL), indicating that higher NaTC concentration can result in the formation of new solubilising species possibly resulting from HPMC-NaTC interaction.

In FaSSIF, with the presence of LT, PXM solubility further raises with respect to B-FaSSIF, highlighting a solubilisation effect played by lecithin on the crystalline drug. However, no significant difference in the drug solubility is observed when HPMC is present. Finally, FeSSIF shows relevantly lower solubilisation effect than B-FeSSIF on PXM alone and PXM with 2 and 4 mg/mL HPMC. When 9 mg/mL HPMC was added, the drug solubility in FeSSIF is higher than the one observed in B-FeSSIF. Obtained results suggest that, although LT does not promote further increase of PXM solubilisation when HPMC is present, it may interfere with the BS-polymer interaction. Thus, these finding suggest a possible alteration of the media colloidal composition, upon interaction and competition between different solubilising aggregates.

3.2. Physicochemical characterisation of the spray dried solid dispersions

To better mimic what happens in the gut, spray dried HPMC-PXM solid dispersions were prepared to assess the impact of the solid dispersion preparation process on the drug solubilisation and HPMC interaction with biorelevant media components. Spray dried samples were characterised using a range of techniques, in order to establish the drug physical state in the formulations. As seen in Fig. 1a, SEM images show that spray dried HPMC and HPMC-PXM solid dispersions are composed of spherical microspheres with particle sizes in the range of 2–10 μm. No significant different in size is observed by changing the drug to polymer ratios.

At a low drug loading (HPMC:PXM 9:1), the microspheres appear to have smooth surfaces and there is no detectable drug melting by DSC (Fig. 1b). For the formulations with higher drug loadings (HPMC:PXM 2:1 and 4:1), some fine needle-shaped crystalline particles can be observed, indicating the likelihood of drug recrystallisation (Fig. 1a). This is confirmed by the DSC results in Fig. 1b that shows detectable drug melting in spray dried microspheres with polymer:drug ratios of 2:1 and 4:1 in the range 187–192 °C. The presence of the recrystallised drug in 2:1 and 4:1 formulations were further confirmed by PXRD and ATR-FTIR results (see Supplementary Material Figure S.1). Drug recrystallisation in the dispersions with higher drug loadings could be attributed to the limited intermolecular interactions between PXM and HPMC which led to poor drug-polymer miscibility. Overall, the physical characterisation results confirmed that at HPMC:PXM ratio of 9:1, an amorphous molecular dispersion was formed, and at 4:1 and 2:1 drug recrystallisation occurred.

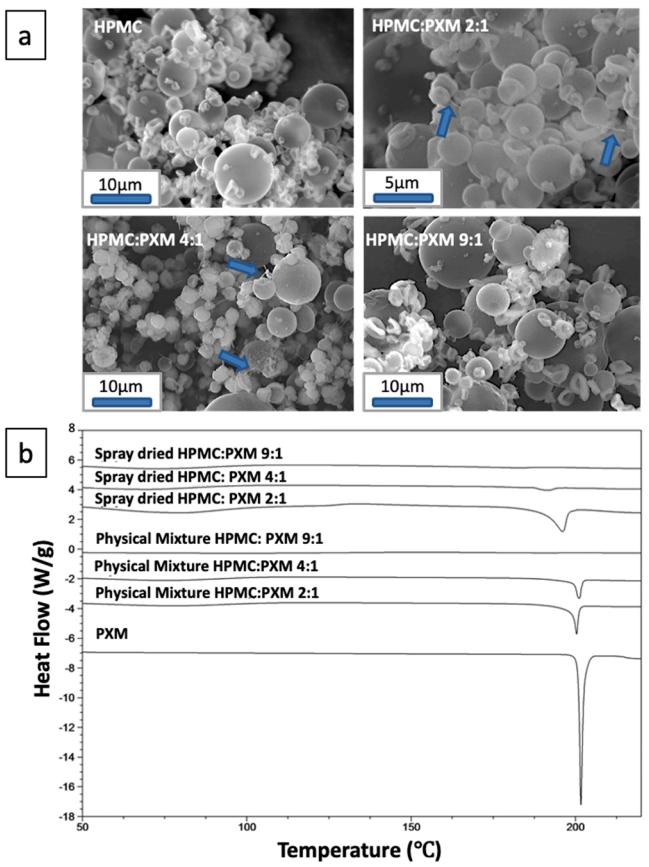

Fig. 1. (a) SEM images of spray dried HPMC, HPMC:PXM 2:1, HPMC:PXM 4:1, HPMC:PXM 9:1 microparticles. Blue arrows indicate PXM crystals. (b) DSC thermograms of raw PXM, HPMC:PXM 2:1, 4:1 and 9:1 physical mixtures and spray dried HPMC:PXM 2:1, 4:1 and 9:1 samples.

3.3. Investigation into the formation of HPMC-NaTC complexes

Solubility studies indicated the impact of HPMC and HPMC based solid dispersion on the solubilisation of PXM, in the presence of NaTC in the biorelevant media. Therefore, we hypothesized that the possible occurrence of interactions between NaTC, LT and HPMC may facilitate the drug dissolution enhancement. DLS and NTA techniques were employed to probe the formation of colloidal species that could play a role as solubilising aggregates, upon dissolution of the spray dried HPMC and formulation HPMC:PXM 2:1 in the employed buffers and media.

First, the self-association behaviour of spray dried HPMC was investigated. As shown by Fig. 2a, DLS data for spray dried HPMC in pH 6.5 buffer show the presence of two populations of aggregates. The bimodal distribution is in good agreement with literature data, which describe the formation of two populations of HPMC aggregates even in highly diluted regimes [64]. The smaller population of HPMC aggregates is characterised by a size of 40 ± 9 d.nm, while the bigger population is 231 ± 45 d.nm in size (Fig. 2a and Supplementary Material Table S.5).

Changing the pH to 5 did not lead to a significant variation in the particle population with a smaller size (see Supplementary Materials Table S.5), but an increase in the relaxation time could be observed in the particle population with a larger size, indicating the formation of aggregates having higher hydrodynamic size (Fig. 3a). The two buffers present different osmolarity (buffer pH 5 270 mOsmol/Kg, buffer pH 5 670 mOsmol/Kg) and the salt contents can influence polymer aggregation *via* salting-in and salting-out effect [65]. This could impact the hydration of the polymeric chains, the hydration sphere of polymeric aggregates and their hydrodynamic size.

DLS measurements of the spray dried HPMC in B-FaSSIF yielded two populations of aggregates with sizes close to the ones obtained for HPMC in pH 6.5 buffer. Such a result shows that the presence of NaTC at a concentration of 3 mM did not significantly influence the aggregation behaviour of HPMC, suggesting a limited interaction between HPMC and NaTC in B-FaSSIF media, as already indicated by solubility studies.

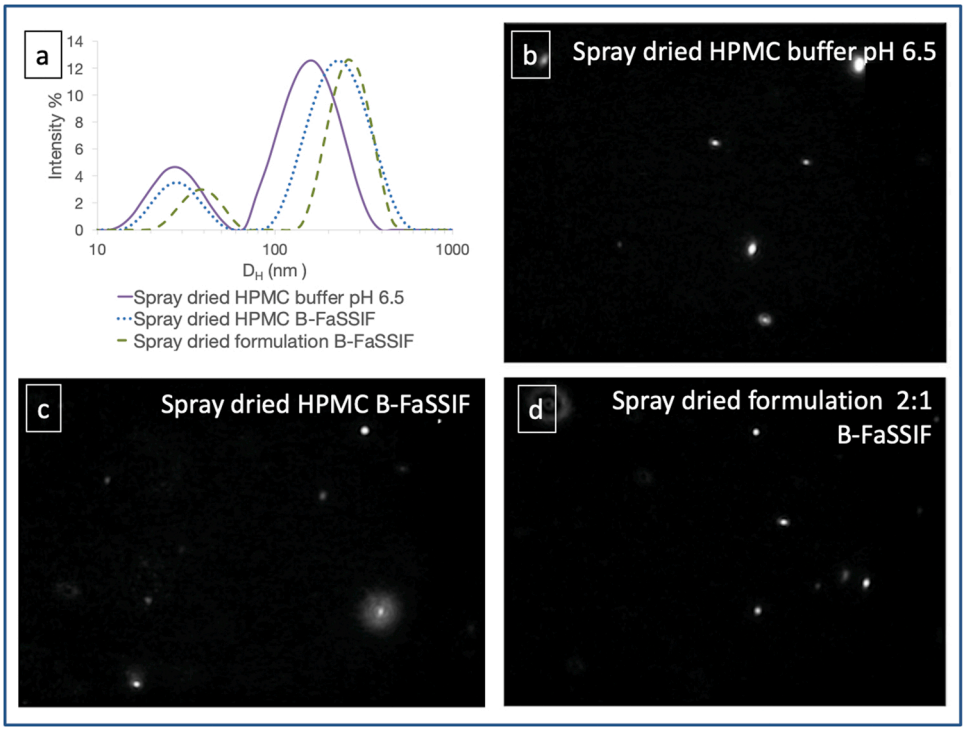

Fig. 2. Intensity-weighed size distribution obtained by (a) DLS and (b-d) their responding scattering aggregates images acquired during Nanosight analysis (NTA) for spray dried HPMC and formulation HPMC:PXM 2:1 samples dissolved in buffer pH 6.5 and B-FaSSIF.

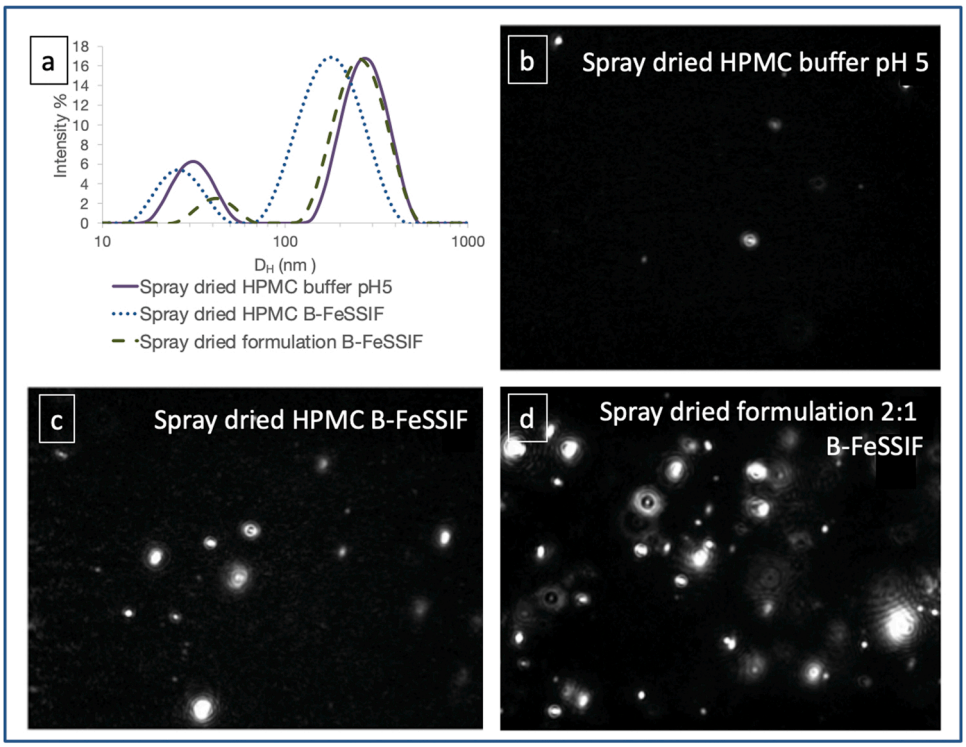

Fig. 3. Intensity-weighed size distribution obtained by (a) DLS and (b-d) their responding scattering aggregates images acquired during Nanosight analysis (NTA) for spray dried HPMC and formulation HPMC:PXM 2:1 samples dissolved in buffer pH 5 and B-FeSSIF.

However, for HPMC in B-FeSSIF, a more significant decrease in the hydrodynamic size of the larger population is seen than the change seen in the population with a smaller size. This indicates that with increasing NaTC concentration, the NaTC-HPMC interaction may lead to changes and/or the formation of mixed surfactant polymer aggregates.

For the dissolved spray-dried formulation 2:1 in B-FaSSIF, an increase in hydrodynamic size was obtained in the bigger population of aggregates (333 ± 59 d.nm measured by DLS). The increase may be due to the swelling of the aggregates associated with the drug encapsulation *via* solubilisation. Such increases are also observed for all drug loaded solid dispersions dissolved in B-FeSSIF. To further study HPMC aggregation behaviour with NaTC, NTA studies were also performed. The rationale of using NTA as an additional complimentary characterisation technique is to be able to direct visualise and study both mono-dispersed and poly-dispersed colloidal systems [66].

As seen in Figs. 2 and 3, a limited number of aggregates were observed for all pH 6.5, pH 5 and B-FaSSIF samples. This result is in agreement with DLS data that showed a weak scattering of HPMC samples in B-FaSSIF, indicating the presence of a low number of aggregates and confirming the limited occurrence of NaTC-HPMC interaction in this medium. When HPMC dissolved in B-FeSSIF, the aggregates with a particle concentration of approximately 5 * 10^6 particle/mL was observed, which is higher than the results obtained for the HPMC dissolved in B-FaSSIF (see Supplementary Materials Figure S.2), revealing the formation of more colloidal solubilising species upon increase of NaTC concentration, as expected. The dissolution of the spray dried solid dispersions led to significant increases in particle concentration and swelling in size of the aggregates, observed using NTA (Fig. 2). This agrees well with DLS results and indicates that the drug solubilisation has an effect on the size of the aggregates. Both DLS and NTA data for all the samples analysed showed broad sizes distribution, indicating the formation of polydispersed aggregates. The high polydispersity is an indication of the formation of a range of nanoscale aggregate species, such as polymer aggregates, polymer/NaTC complexes and free NaTC micelles, and their dynamic formation processing.

In the case of FaSSIF and FeSSIF, the presence of LT led to more complex composition of the solutions, with dissolved formulations resulting in less resolved particle size distribution by DLS measurements (as seen in Supplementary Materials Figure S.3). LT and NaTC can interact leading to the formation of a variety of nanoaggregates, according to NaTC concentration [67,68]. In this case, the occurrence of interaction between HPMC and NaTC can interfere the NaTC-LT interaction, yielding an even wider variety of aggregated structures. In particular, the dissolution of the spray dried HPMC:PXM in FaSSIF formulation led to a wide size distribution, with a peak centred at 330 ± 73 nm (as shown in Supplementary Materials Fig. S3 and Table S.5). The high polydispersity reflects the heterogeneity of the scattering from the nanoaggregates, which most likely include NaTC-LT vesicles, NaTC micelle, HPMC-NaTC monomers complexes and HPMC aggregates. The size distribution of the spray dried formulation dissolved in FeSSIF presents two peaks, that correspond to two scattering aggregates populations similar to the ones measured in B-FeSSIF and B-FaSSIF. As previously reported, in FeSSIF NaTC-LT micelles are formed [69]. In this case, as NaTC is well above its CMC in FeSSIF, the presence NaTC monomer is unlikely and the presence of HPMC may lead to the formation of HPMC-NaTC-LT micellar complexes.

The colloidal composition of spray dried HPMC:PXM 2:1 formulation dissolved in B-FeSSIF was further studied using Cryo-TEM. The NTA data of the formulation in B-FaSSIF indicated a low concentration of aggregates (1.4 * 10^6 particles/mL), which was unsuitable for Cryo-TEM imaging (see Supplementary Material Figure S.2). For spray dried HPMC dissolved in B-FeSSIF, Cryo-TEM micrographs (Fig. 4 a and b) show the presence of globular micelles having a diameter of 10 nm. NaTC, as other BS, is characterised by very low aggregation number (N_{agg} = 2–15) and is known to assemble into highly dynamic micelles having a few nanometres size, that, although influenced by the presence of salts, is usually in the range of 2–3 nm [42]. Given the surface activity of HPMC and its ability to interact with NaTC [49,70], we speculate that the globular micelles observed in Fig. 4 a and b might be HPMC-NaTC complexes that co-exist alongside with NaTC micelles.

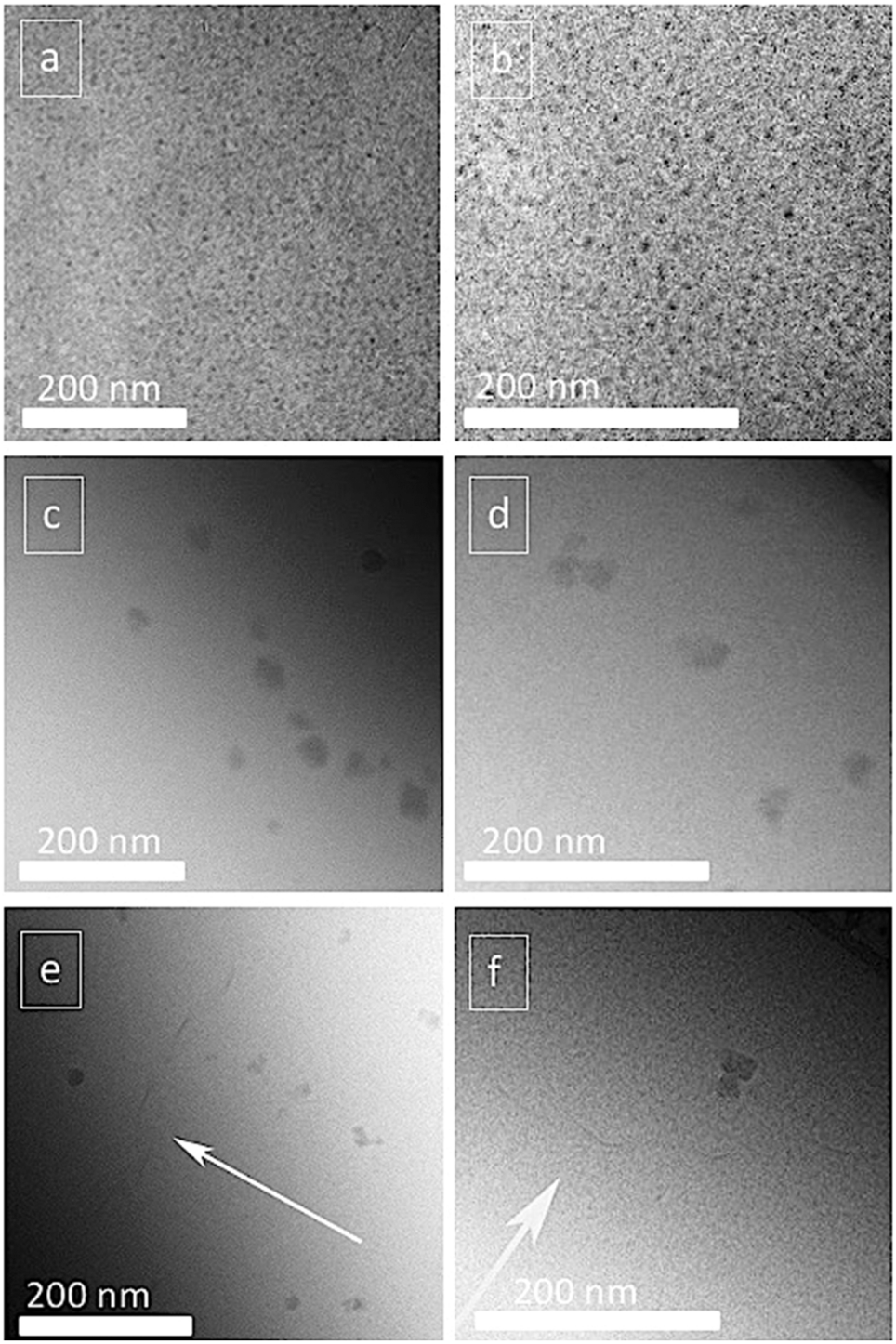

Fig. 4. Cryo-TEM micrographs of spray dried HPMC (a and b) and spray dried formulation HPMC:PXM 2:1 (c-f) dissolved in B-FeSSIF. Arrows indicate twisted thread-like structures.

For the solution of spray dried HPMC:PXM 2:1 dissolved in B-FeSSIF, Cryo-TEM analysis revealed a different colloidal composition with the formation of fuzzy aggregates having a diameter of about 25 nm, as showed in Fig. 4 c and d, which could possible correspond to the smaller population observed in DLS data (hydrodynamic size 52 ± 10 nm). Moreover, the sample was characterised by the presence of twisted thread-like structures having a length of about 300 nm, that could be identified as HPMC thread-like micelles (Fig. 4 e and f), which formation by cellulose ethers has already been described in the literature [70]. Such nanostructures could be associated with the bigger-sized population observed for this sample by DLS (hydrodynamic size 423 ± 70 nm). These results agree well with DLS and NTA results and further indicated that the presence of PXM clearly impacted the system self-assembly and suggested that the possible drug encapsulation/solubilisation within the HPMC-NaTC complexes which might lead to the formation of the aggregates with larger size.

3.4. Drug uptake study using Caco-2 model cell line

In order to evaluate the impact of polymers and other components in

the biorelevant media on the passively drug absorption [71], PXM uptake from the spray dried solid dispersions was studied using Caco-2 as a model cell line. In the existing literature, the use of biorelevant media in Caco-2 transport and absorption studies has been recognised as a useful part of preclinical and pre-*in vivo* studies to enable indicative prediction of drugs absorption *in vivo* [72,73]. However, BSs are known to have a cytotoxic effect that can cause cell membrane damage. Therefore, in this study, in order to establish suitable NaTC concentrations to perform Caco-2 cell experiments using modified B-FaSSIF, B-FeSSIF, FaSSIF and FeSSIF, cytotoxicity studies were performed in the first instance. Two types of assays were used to evaluate the cytotoxicity, LDH and Cyto-Tox Glo™ (see Supplementary Material Sections Tables S6-S10). The results confirmed the cytotoxicity of NaTC being previously reported [52], and the NaTC concentration in the at 1.5 mM showed non-cytotoxic and were used in the drug uptake studies. The modified bio-relevant media without LT are named as B-FeSSIF-2 and B-FaSSIF-2, while the same media in the presence of LT 0.75 mM were labelled FeSSIF-2 and FaSSIF-2.

HPMC did not show any cytotoxicity to Caco-2 cells, which is in agreement with the literature [74]. LT was also shown to be compatible with Caco-2 cells, as no significant cytotoxicity was observed for the solutions with LT concentration of 0.75 mM, which is the same concentration used in FaSSIF. Patel et al. suggested that BS cytotoxicity could be reduced by the presence of LT, as phospholipids have been shown to protect cellular membrane from BSs damage [75,76]. However, no decrease in NaTC cytotoxicity was found in the presence of LT in this study. Interestingly, the decrease of NaTC cytotoxicity was observed in the presence of the spray-dried formulation (see data in Supplementary Materials Tables S.9 and S.10). This reduction may be a consequence of the NaTC-HPMC interaction, which decrease the amount of free NaTC that can interact with membrane lipids and cause the cellular membrane damage. This effect was also confirmed by Cyto-Tox Glo™ assay (see data in Supplementary Materials Tables S.9 and S.10).

As the controls, PXM uptake by Caco-2 was firstly assessed in the media containing DMEM, acetate and phosphate buffers. The influence of NaTC on PXM uptake was investigated by using acetate (pH 5) and phosphate (pH 6.5) buffered NaTC 1.5 mM solutions. The impact of spray drying formulation on the drug uptake was studied using spray dried HPMC:PXM 4:1 solid dispersions. Solid dispersions were dissolved in the acetate and phosphate buffers used in the solubility studies and in NaTC buffered solution with and without the presence of LT. The results from these experiments are summarised in Fig. 5. It can be seen that 17.0 ± 0.4 % of PXM in DMEM was absorbed by Caco-2 cells at the end of 2 h testing period. No significant change in the drug absorption was observed for PXM in acetate (pH 5) and phosphate (pH 6.5) buffers (Fig. 5). This result indicates that, despite the higher solubility of PXM at pH 6.5 shown by solubility studies (Table 2), *in vitro* cellular drug uptake was not affected by the pH of the media.

PXM uptake of the spray-dried formulations in buffer pH 6.5 and pH 5 showed no significant difference. The presence of 1.5 mM of NaTC in the solutions (B-FaSSIF-2 and B-FeSSIF-2) did not lead to significant uptake increase, indicating the minor role NaTC played in enhancing drug absorption by Caco-2 cells at the concentration used. This is not surprising as the NaTC concentration was kept significantly lower than its CMC and the ones used in the solubility study (due to the cellular cytotoxicity issues). This should be taking into consideration when analysing the following data on FaSSIF-2 and FeSSIF-2 media.

The PXM uptakes were further increased when FaSSIF-2 and FeSSIF-2 were used as the media. This is in good agreement with steady state solubility results that showed the highest PXM solubilisation in FaSSIF, confirming the potential contribution of LT in enhancing drug solubility and subsequent uptake. Despite the limitation of the compositions of the modified media (lower NaTC concentration than the ones used in the standard FeSSIF and FaSSIF media) used in the Caco-2 cell studies, the results of the cellular uptake studies support the hypothesis that the occurrence of HPMC-NaTC aggregation may play a role in the absorption of poorly water-soluble drugs in the gastrointestinal tract. Indeed, the highest uptake of PXM was obtained when both polymeric carrier and simulated intestinal media were used in the tests.

4. Conclusions

This study investigated the impact of polymer, the formation of solid dispersion and the presence of NaTC on the solubility and Caco-2 cellular uptake of a model poorly water-soluble drug, PXM. The addition of HPMC, even as a physical mixture, showed significant impact on drug steady state solubility. DLS and NTA studies suggested the possible formation of HPMC-NaTC aggregates that may play a role in the model drug solubilisation. Significant decrease of NaTC cytotoxic was observed with the addition of HPMC. The results of the cellular drug uptake studies showed higher PXM uptake from spray dried solid dispersion formulation in FeSSIF-2 and FaSSIF-2 which indirectly supported the hypothesis of the possible occurrence of the HPMC-NaTC interaction having a role to play in drug solubilisation and absorption *in vivo* for polymeric solid dispersions. These findings highlighted the importance of biorelevant media in solid dispersion studies and the key role of the colloidal species formed during dissolution processes in the drug solubilisation and uptake. Further studies on the colloidal compositions of biorelevant media upon dissolution of polymeric solid dispersion will be carried out to complete the understanding on the solubilisation process of poorly soluble drugs delivered by polymeric solid dispersions.

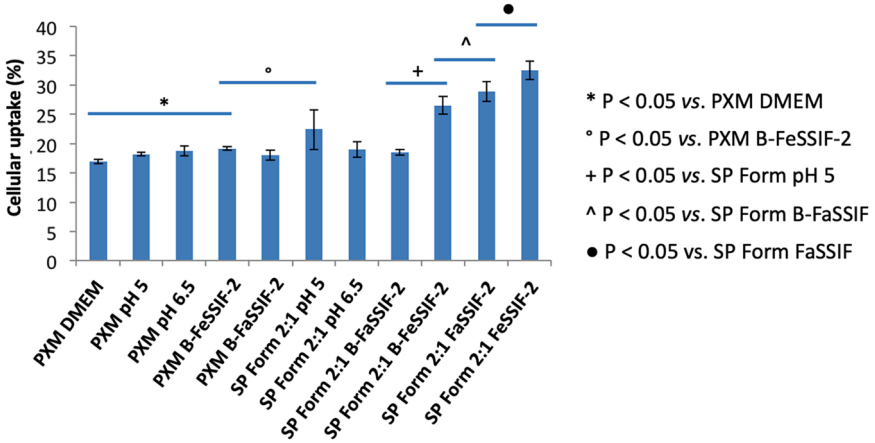

Fig. 5. Caco-2 cellular uptake studies results for raw PXM raw and the spray dried solid dispersion formulation (SP Form) HPMC:PXM 4:1 in different media. (n = 5).

CRediT authorship contribution statement

Claudia Pigliacelli: Data curation, Investigation, Visualisation, Methodology, Writing – original draft, Writing – review & editing. **Peter Belton:** Conceptualization, Methodology, Writing – review & editing. **Peter Wilde:** Conceptualization, Methodology, Supervision, Writing – review & editing. **Francesca Baldelli Bombelli:** Conceptualization, Methodology, Writing – review & editing. **Paul A Kroon:** Resources, Methodology, Investigation, Supervision, Writing – review & editing. **Mark S Winterbone:** Resources, Methodology, Investigation, Writing – review & editing. **Sheng Qi:** Conceptualization, Funding acquisition, Methodology, Project administration, Resources, Supervision, Writing – original draft, Writing – review & editing.

Declaration of Competing Interest

The authors declare that they have no known competing financial interests or personal relationships that could have appeared to influence the work reported in this paper.

Data availability

Data will be made available on request.

Acknowledgments

The authors would like to thank the University of East Anglia for the PhD studentship funding and the Biotechnology and Biological Sciences Research Council (BBSRC) for supporting this research through an Institute Strategic Programme Grant (Food Innovation and Health, BB/R012512/1) and its constituent project(s) BBS/E/F/000PR10343 (Theme 1, Food Innovation) and BBS/E/F/000PR10345 (Theme 2, Digestion in the Upper GI Tract).

Appendix A. Supporting information

Supplementary data associated with this article can be found in the online version at doi:10.1016/j.colsurfb.2022.113044.

References

[1] P. Gunness, B.M. Flanagan, M.J. Gidley, Molecular interactions between cereal soluble dietary fibre polymers and a model bile salt deduced from ^{13}C NMR titration, J. Cereal Sci. 52 (2010) 444–449, https://doi.org/10.1016/j.jcs.2010.07.009.

[2] G.L. Amidon, H. Lennernäs, V.P. Shah, J.R. Crison, Theoretical basis for a biopharmaceutic drug classification: the correlation of in vitro drug product dissolution and in vivo bioavailability, Pharm. Res. 12 (1995) 413–420, https://doi.org/10.1023/A:1016212804288.

[3] A. Dokoumetzidis, P. Macheras, A century of dissolution research: from Noyes and Whitney to the biopharmaceutics classification system, Int. J. Pharm. 321 (2006) 1–11, https://doi.org/10.1016/j.ijpharm.2006.07.011.

[4] C.W. Pouton, Formulation of poorly water-soluble drugs for oral administration: physicochemical and physiological issues and the lipid formulation classification system. Eur. J. Pharm. Sci. 29 (2006) 278–287, https://doi.org/10.1016/j.ejps.2006.04.016.

[5] H.D. Williams, N.L. Trevaskis, S.A. Charman, R.M. Shanker, W.N. Charman, C. W. Pouton, C.J.H. Porter, Strategies to address low drug solubility in discovery and development, Pharmacol. Rev. 65 (2013) 315–499. ⟨http://www.ncbi.nlm.nih.gov/pubmed/23383426⟩. accessed August 30, 2014.

[6] K. Kogermann, A. Penkina, K. Predbannikova, K. Jeeger, P. Veski, J. Rantanen, K. Naelapää, Dissolution testing of amorphous solid dispersions, Int. J. Pharm. 444 (2013) 40–46, https://doi.org/10.1016/j.ijpharm.2013.01.042.

[7] T. Vasconcelos, B. Sarmento, P. Costa, Solid dispersions as strategy to improve oral bioavailability of poor water soluble drugs, Drug Discov. Today 12 (2007) 1068–1075, https://doi.org/10.1016/j.drudis.2007.09.005.

[8] Y.K. Choi, B.K. Poudel, N. Marasini, K.Y. Yang, J.W. Kim, J.O. Kim, H.-G. Choi, C. S. Yong, Enhanced solubility and oral bioavailability of itraconazole by combining membrane emulsification and spray drying technique. Int. J. Pharm. 434 (2012) 264–271, https://doi.org/10.1016/j.ijpharm.2012.05.039.

[9] C. Leuner, Improving drug solubility for oral delivery using solid dispersions, Eur. J. Pharm. Biopharm. 50 (2000) 47–60, https://doi.org/10.1016/S0939-6411(00)00076-X.

[10] A.T. Serajuddin, Solid dispersion of poorly water-soluble drugs: early promises, subsequent problems, and recent breakthroughs., J. Pharm. Sci. 88 (1999) 1058–66. http://www.ncbi.nlm.nih.gov/pubmed/10514356 (accessed May 29, 2014).

[11] Y. Huang, W.-G. Dai, Fundamental aspects of solid dispersion technology for poorly soluble drugs, Acta Pharm. Sin. B 4 (2014) 18–25, https://doi.org/10.1016/j.apsb.2013.11.001.

[12] C.A.S. Bergström, R. Holm, S.A. Jørgensen, S.B.E. Andersson, P. Artursson, S. Beato, A. Borde, K. Box, M. Brewster, J. Dressman, K.I. Feng, G. Halbert, E. Kostewicz, M. McAllister, U. Muenster, J. Thinnes, R. Taylor, A. Mullertz, Early pharmaceutical profiling to predict oral drug absorption: current status and unmet needs, Eur. J. Pharm. Sci. 57 (2014) 173–199, https://doi.org/10.1016/j.ejps.2013.10.015.

[13] M. Koziolek, M. Grimm, F. Schneider, P. Jedamzik, M. Sager, J.P. Kühn, W. Siegmund, W. Weitschies, Navigating the human gastrointestinal tract for oral drug delivery: uncharted waters and new frontiers, Adv. Drug Deliv. Rev. 101 (2016) 75–88, https://doi.org/10.1016/j.addr.2016.03.009.

[14] E.S. Kostewicz, B. Abrahamsson, M. Brewster, J. Brouwers, J. Butler, S. Carlert, P. A. Dickinson, J. Dressman, R. Holm, S. Klein, J. Mann, M. McAllister, M. Minekus, U. Muenster, A. Müllertz, M. Verwei, M. Vertzoni, W. Weitschies, P. Augustijns, In vitro models for the prediction of in vivo performance of oral dosage forms, Eur. J. Pharm. Sci. 57 (2014) 342–366, https://doi.org/10.1016/j.ejps.2013.08.024.

[15] B.J. Boyd, C.A.S. Bergström, Z. Vinarov, M. Kuentz, J. Brouwers, P. Augustijns, M. Brandl, A. Bernkop-Schnürch, N. Shrestha, V. Préat, A. Müllertz, A. Bauer-Brandl, V. Jannin, Successful oral delivery of poorly water-soluble drugs both depends on the intraluminal behavior of drugs and of appropriate advanced drug delivery systems, Eur. J. Pharm. Sci. 137 (2019), 104967, https://doi.org/10.1016/j.ejps.2019.104967.

[16] N. Pavlović, S. Goločorbin-Kon, M. Đanić, B. Stanimirov, H. Al-Salami, K. Stankov, M. Mikov, Bile acids and their derivatives as potential modifiers of drug release and pharmacokinetic profiles, Front. Pharmacol. 9 (2018) 1283, https://doi.org/10.3389/fphar.2018.01283.

[17] Z. Vinarov, V. Katev, N. Burdzhiev, S. Tcholakova, N. Denkov, Effect of surfactant-bile interactions on the solubility of hydrophobic drugs in biorelevant dissolution media, Mol. Pharm. 15 (2018) 5741–5753, https://doi.org/10.1021/acs.molpharmaceut.8b00884.

[18] J. Wiest, M. Saedtler, B. Böttcher, M. Grüne, M. Reggane, B. Galli, U. Holzgrabe, L. Meinel, Geometrical and structural dynamics of imatinib within biorelevant colloids, Mol. Pharm. 15 (2018) 4470–4480, https://doi.org/10.1021/acs.molpharmaceut.8b00469.

[19] W.N. Charman, C.J. Porter, S. Mithani, J.B. Dressman, Physiochemical and physiological mechanisms for the effects of food on drug absorption: the role of lipids and pH. J. Pharm. Sci. 86 (1997) 269–282, https://doi.org/10.1021/js960085v.

[20] R. Holm, A. Mullertz, H. Mu, Bile salts and their importance for drug absorption, Int. J. Pharm. 453 (2013) 44–55, https://doi.org/10.1016/j.ijpharm.2013.04.003.

[21] G.A. Haslewood, Bile Salts, Richard Clay Ltd, 1967.

[22] J. Maldonado-Valderrama, P. Wilde, A. Macierzanka, A. Mackie, The role of bile salts in digestion, Adv. Colloid Interface Sci. 165 (2011) 36–46, https://doi.org/10.1016/j.cis.2010.12.002.

[23] J.B. Dressman, G.L. Amidon, C. Reppas, V.P. Shah, Dissolution testing as a prognostic tool for oral drug absorption: immediate release dosage forms, Pharm. Res. 15 (1998) 11–22, https://doi.org/10.1023/A:1011984216775.

[24] E. Galia, E. Nicolaides, D. Hörter, R. Löbenberg, C. Reppas, J.B. Dressman, Evaluation of various dissolution media for predicting in vivo performance of class I and II drugs, Pharm. Res. 15 (1998) 698–705, https://doi.org/10.1023/a:1011910801212.

[25] A. Fuchs, M. Leigh, B. Kloefer, J.B. Dressman, Advances in the design of fasted state simulating intestinal fluids: FaSSIF-V3, Eur. J. Pharm. Biopharm. 94 (2015) 229–240, https://doi.org/10.1016/j.ejpb.2015.05.015.

[26] L. Klumpp, M. Leigh, J. Dressman, Dissolution behavior of various drugs in different FaSSIF versions, Eur. J. Pharm. Sci. 142 (2020), 105138, https://doi.org/10.1016/j.ejps.2019.105138.

[27] I. Loisios-Konstantinidis, R. Cristofoletti, N. Fotaki, D.B. Turner, J. Dressman, Establishing virtual bioequivalence and clinically relevant specifications using in vitro biorelevant dissolution testing and physiologically-based population pharmacokinetic modeling. case example: Naproxen, Eur. J. Pharm. Sci. 143 (2020), 105170, https://doi.org/10.1016/j.ejps.2019.105170.

[28] T. Winuprasith, S. Chantarak, M. Suphantharika, L. He, D.J. McClements, Alterations in nanoparticle protein corona by biological surfactants: Impact of bile salts on β-lactoglobulin-coated gold nanoparticles, J. Colloid Interface Sci. 426 (2014) 333–340, https://doi.org/10.1016/j.jcis.2014.04.018.

[29] B.K. Paul, N. Ghosh, S. Mukherjee, Direct insight into the nonclassical hydrophobic effect in bile salt:β-cyclodextrin interaction: Role of hydrophobicity in governing the prototropism of a biological photosensitizer, RSC Adv. 6 (2016) 9984–9993, https://doi.org/10.1039/c5ra27050b.

[30] M.S. Mikkelsen, S.B. Cornali, M.G. Jensen, M. Nilsson, S.R. Beeren, S. Meier, Probing interactions between β-glucan and bile salts at atomic detail by1h-^{13}C NMR assays, J. Agric. Food Chem. 62 (2014) 11472–11478, https://doi.org/10.1021/jf504352w.

[31] X. Wang, M. Fan, Interaction behaviors and structural characteristics of zein/NaTC nanoparticles, RSC Adv. 9 (2019) 5748–5755, https://doi.org/10.1039/c9ra00005d.

[32] E. Tasca, A. Del Giudice, L. Galantini, K. Schillén, A.M. Giuliani, M. Giustini, A fluorescence study of the loading and time stability of doxorubicin in sodium

cholate/PEO-PPO-PEO triblock copolymer mixed micelles, J. Colloid Interface Sci. 540 (2019) 593–601, https://doi.org/10.1016/j.jcis.2019.01.075.
[33] E. Tasca, P. Andreozzi, A. Del Giudice, L. Galantini, K. Schillén, A. Maria Giuliani, M. de los A. Ramirez, S.E. Moya, M. Giustini, Poloxamer/sodium cholate co-formulation for micellar encapsulation of doxorubicin with high efficiency for intracellular delivery: an in-vitro bioavailability study, J. Colloid Interface Sci. 579 (2020) 551–561, https://doi.org/10.1016/j.jcis.2020.06.096.
[34] A. Hammarström, L.-O. Sundelöf, NMR study of polymer surfactant interaction in the system HPMC/SDS/water, Colloid Polym. Sci. 271 (1993) 1129–1133, https://doi.org/10.1007/BF00657067.
[35] P. Hansson, B. Lindman, Surfactant-polymer interactions, Curr. Opin. Colloid Interface Sci. 1 (1996) 604–613, https://doi.org/10.1016/S1359-0294(96)80098-7.
[36] J.-E. Löfroth, L. Johansson, A.-C. Norman, K. Wettström, Interactions between surfactants and polymers. II: polyelectrolytes, in: M. Corti, F. Mallamace (Eds.), Trends Colloid Interface Sci. V, Steinkopff, Darmstadt, 2007, pp. 78–82, https://doi.org/10.1007/bfb0115939.
[37] V. Patel, D. Ray, A. Bahadur, J. Ma, V.K. Aswal, P. Bahadur, Pluronic®-bile salt mixed micelles, Colloids Surf. B Biointerfaces 166 (2018) 119–126, https://doi.org/10.1016/j.colsurfb.2018.03.001.
[38] C. Chakrabarti, N. Malek, D. Ray, V.K. Aswal, S.A. Pillai, A meticulous study on the interaction of bile salts with star block copolymeric micelles, J. Mol. Liq. 363 (2022), 119877, https://doi.org/10.1016/j.molliq.2022.119877.
[39] K. Schillén, L. Galantini, G. Du, A. Del Giudice, V. Alfredsson, A.M. Carnerup, N. V. Pavel, G. Masci, B. Nyström, Block copolymers as bile salt sequestrants: Intriguing structures formed in a mixture of an oppositely charged amphiphilic block copolymer and bile salt, Phys. Chem. Chem. Phys. 21 (2019) 12518–12529, https://doi.org/10.1039/c9cp01744e.
[40] S. Bayati, L. Galantini, K.D. Knudsen, K. Schillén, Complexes of PEO-PPO-PEO triblock copolymer P123 and bile salt sodium glycodeoxycholate in aqueous solution: a small angle X-ray and neutron scattering investigation, Colloids Surf. A Physicochem. Eng. Asp. 504 (2016) 426–436, https://doi.org/10.1016/j.colsurfa.2016.05.096.
[41] S. Bayati, L. Galantini, K.D. Knudsen, K. Schillén, Effects of bile salt sodium glycodeoxycholate on the self-assembly of PEO-PPO-PEO triblock copolymer P123 in aqueous solution, Langmuir 31 (2015) 13519–13527, https://doi.org/10.1021/acs.langmuir.5b03828.
[42] G. Du, D. Belić, A. Del Giudice, V. Alfredsson, A.M. Carnerup, K. Zhu, B. Nyström, Y. Wang, L. Galantini, K. Schillén, Condensed supramolecular helices: the twisted sisters of DNA, Angew. Chem. 134 (2022) 1–8, https://doi.org/10.1002/ange.202113279.
[43] J. Schlauersbach, S. Hanio, B. Lenz, S.P.B. Vemulapalli, C. Griesinger, A.C. Pöppler, C. Harlacher, B. Galli, L. Meinel, Leveraging bile solubilization of poorly water-soluble drugs by rational polymer selection, J. Control. Release 330 (2021) 36–48, https://doi.org/10.1016/j.jconrel.2020.12.016.
[44] C. Pigliacelli, P. Belton, P. Wilde, S. Qi, Probing the molecular interactions between pharmaceutical polymeric carriers and bile salts in simulated gastrointestinal fluids using NMR spectroscopy, J. Colloid Interface Sci. 551 (2019) 147–154, https://doi.org/10.1016/j.jcis.2019.05.002.
[45] D.J.F. Taylor, R.K. Thomas, J. Penfold, Polymer/surfactant interactions at the air/water interface, Adv. Colloid Interface Sci. 132 (2007) 69–110, https://doi.org/10.1016/j.cis.2007.01.002.
[46] S. Banerjee, C. Cazeneuve, N. Baghdadli, S. Ringeissen, F.A.M. Leermakers, G. S. Luengo, Surfactant-polymer interactions: molecular architecture does matter, Soft Matter 11 (2015) 2504–2511, https://doi.org/10.1039/c5sm00117j.
[47] C.La Mesa, Polymer-surfactant and protein-surfactant interactions, J. Colloid Interface Sci. 286 (2005) 148–157, https://doi.org/10.1016/j.jcis.2004.12.038.
[48] T.M. Deshpande, H. Shi, J. Pietryka, S.W. Hoag, A. Medek, Investigation of polymer/surfactant interactions and their impact on itraconazole solubility and precipitation kinetics for developing spray-dried amorphous solid dispersions, Mol. Pharm. 15 (2018) 962–974, https://doi.org/10.1021/acs.molpharmaceut.7b00902.
[49] S. Qi, S. Roser, K.J. Edler, C. Pigliacelli, M. Rogerson, I. Weuts, F. Van Dycke, S. Stokbroekx, Insights into the role of polymer-surfactant complexes in drug solubilisation/stabilisation during drug release from solid dispersions, Pharm. Res. 30 (2013) 290–302, https://doi.org/10.1007/s11095-012-0873-7.
[50] I.E. Shohin, J.I. Kulinich, G.V. Ramenskaya, B. Abrahamsson, S. Kopp, P. Langguth, J.E. Polli, V.P. Shah, D.W. Groot, D.M. Barends, J.B. Dressman, Biowaiver monographs for immediate release solid oral dosage forms: piroxicam, J. Pharm. Sci. 103 (2014) 367–377, https://doi.org/10.1002/jps.23799.
[51] Y.S.R. Elnaggar, Multifaceted applications of bile salts in pharmacy: an emphasis on nanomedicine, Int. J. Nanomed. 10 (2015) 3955–3971, https://doi.org/10.2147/IJN.S82558.
[52] M. Marques, Dissolution media simulating fasted and fed states, Dissolution Technol. 11 (2004), https://doi.org/10.14227/DT110204P16.
[53] P. Vinson, J. Bellare, H. Davis, W. Miller, L. Scriven, Direct imaging of surfactant micelles, vesicles, discs, and ripple phase structures by cryo-transmission electron microscopy, J. Colloid Interface Sci. 142 (1991) 74–91, https://doi.org/10.1016/0021-9797(91)90034-6.
[54] C. Korzeniewski, D.M. Callewaert, An enzyme-release assay for natural cytotoxicity, J. Immunol. Methods 64 (1983) 313–320, https://doi.org/10.1016/0022-1759(83)90438-6.
[55] H.-S. Gwak, J.-S. Choi, H.-K. Choi, Enhanced bioavailability of piroxicam via salt formation with ethanolamines. Int. J. Pharm. 297 (2005) 156–161, https://doi.org/10.1016/j.ijpharm.2005.03.016.
[56] Yu Shin, Ji Lee, Han Joung, Kang Yoo, A hydroxypropyl methylcellulose-based solid dispersion of curcumin with enhanced bioavailability and its hepatoprotective activity, Biomolecules 9 (2019) 281, https://doi.org/10.3390/biom9070281.
[57] N. Fan, Z. He, P. Ma, X. Wang, C. Li, J. Sun, Y. Sun, J. Li, Impact of HPMC on inhibiting crystallization and improving permeability of curcumin amorphous solid dispersions, Carbohydr. Polym. 181 (2018) 543–550, https://doi.org/10.1016/j.carbpol.2017.12.004.
[58] S.A. Mitchell, T.D. Reynolds, T.P. Dasbach, A compaction process to enhance dissolution of poorly water-soluble drugs using hydroxypropyl methylcellulose, Int. J. Pharm. 250 (2003) 3–11, https://doi.org/10.1016/S0378-5173(02)00293-4.
[59] J.M. Ting, W.W. Porter, J.M. Mecca, F.S. Bates, T.M. Reineke, Advances in polymer design for enhancing oral drug solubility and delivery, Bioconjug. Chem. 29 (2018) 939–952, https://doi.org/10.1021/acs.bioconjchem.7b00646.
[60] J. Bevernage, T. Forier, J. Brouwers, J. Tack, P. Annaert, P. Augustijns, Excipient-mediated supersaturation stabilization in human intestinal fluids, Mol. Pharm. 8 (2011) 564–570, https://doi.org/10.1021/mp100377m.
[61] D. Caccavo, G. Lamberti, A.A. Barba, S. Abrahmsén-Alami, A. Viridén, A. Larsson, Effects of HPMC substituent pattern on water up-take, polymer and drug release: an experimental and modelling study, Int. J. Pharm. 528 (2017) 705–713, https://doi.org/10.1016/j.ijpharm.2017.06.064.
[62] E. Leyk, M. Wesolowski, Interactions between paracetamol and hypromellose in the solid state, Front. Pharmacol. 10 (2019) 1–11, https://doi.org/10.3389/fphar.2019.00014.
[63] V. Bakatselou, R.C. Oppenheim, J.B. Dressman, Solubilization and wetting effects of bile salts on the dissolution of steroids, Pharm. Res. 8 (1991) 1461–1469, https://doi.org/10.1023/A:1015877929381.
[64] S. Nilsson, Interactions between water-soluble cellulose derivatives and surfactants. 1. The HPMC/SDS/Water system, Macromolecules 28 (1995) 7837–7844, https://doi.org/10.1021/ma00127a034.
[65] S.C. Joshi, Sol-gel behavior of hydroxypropyl methylcellulose (HPMC) in ionic media including drug release, Materials (Basel) 4 (2011) 1861–1905, https://doi.org/10.3390/ma4101861.
[66] A. Malloy, Count, size and visualize nanoparticles, Mater. Today 14 (2011) 170–173, https://doi.org/10.1016/S1369-7021(11)70089-X.
[67] D. Madenci, A. Salonen, P. Schurtenberger, J.S. Pedersen, S.U. Egelhaaf, Simple model for the growth behaviour of mixed lecithin-bile salt micelles, Phys. Chem. Chem. Phys. 13 (2011) 3171–3178, https://doi.org/10.1039/c0cp01700k.
[68] C.-Y. Cheng, H. Oh, T.-Y. Wang, S.R. Raghavan, S.-H. Tung, Mixtures of lecithin and bile salt can form highly viscous wormlike micellar solutions in water, Langmuir 30 (2014) 10221–10230, https://doi.org/10.1021/la502380q.
[69] A.J. Clulow, A. Parrow, A.M. Hawley, J. Khan, A. Pham, P. Larsson, C.A. S. Bergström, B.J. Boyd, Characterization of solubilizing nanoaggregates present in different versions of simulated intestinal fluid, J. Phys. Chem. B. 121 (2017) 10869–10881, https://doi.org/10.1021/acs.jpcb.7b08622.
[70] R. Bodvik, A. Dedinaite, L. Karlson, M. Bergström, P. Bäverbäck, J.S. Pedersen, K. Edwards, G. Karlsson, I. Varga, P.M. Claesson, Aggregation and network formation of aqueous methylcellulose and hydroxypropylmethylcellulose solutions, Colloids Surf. A Physicochem. Eng. Asp. 354 (2010) 162–171, https://doi.org/10.1016/j.colsurfa.2009.09.040.
[71] E. Walter, S. Janich, B.J. Roessler, J.M. Hilfinger, G.L. Amidon, HT29-MTX/Caco-2 cocultures as an in vitro model for the intestinal epithelium: in vitro-in vivo correlation with permeability data from rats and humans. J. Pharm. Sci. 85 (1996) 1070–1076, https://doi.org/10.1021/js960110x.
[72] F. Ingels, B. Beck, M. Oth, P. Augustijns, Effect of simulated intestinal fluid on drug permeability estimation across Caco-2 monolayers. Int. J. Pharm. 274 (2004) 221–232, https://doi.org/10.1016/j.ijpharm.2004.01.014.
[73] F. Ingels, S. Deferme, E. Destexhe, M. Oth, G. Van den Mooter, P. Augustijns, Simulated intestinal fluid as transport medium in the Caco-2 cell culture model, Int. J. Pharm. 232 (2002) 183–192, https://doi.org/10.1016/S0378-5173(01)00897-3.
[74] B.D. Rege, L.X. Yu, A.S. Hussain, J.E. Polli, Effect of common excipients on Caco-2 transport of low-permeability drugs. J. Pharm. Sci. 90 (2001) 1776–1786. (http://www.ncbi.nlm.nih.gov/pubmed/11745735).
[75] G.P. Martin, C. Marriott, Membrane damage by bile salts: the protective function of phospholipids, J. Pharm. Pharmacol. 33 (1981) 754–759, https://doi.org/10.1111/j.2042-7158.1981.tb13926.x.
[76] N. Patel, B. Forbes, S. Eskola, J. Murray, Use of simulated intestinal fluids with Caco-2 cells and rat ileum, Drug Dev. Ind. Pharm. 32 (2006) 151–161, https://doi.org/10.1080/03639040500465991.